Understanding cosmological observables via numerical simulation of CMB anisotropies

AST5220: Cosmology II

Candidate 15003

Institute of Theoretical Astrophysics, University of Oslo, 0315 Oslo, Norway

Received June 1, 2025

ABSTRACT

Context. The Cosmic Microwave Background (CMB) gives us a way to observationally probe the early development of the Universe.
Aims. Develop cosmological simulations that can test different parameter combinations against observational results. Understand results from modern cosmology.
Methods. Code developed in C++, similar to CAMB or CLASS.
Results. A matter power spectrum and a CMB power spectrum, which can be plotted and compared to observational data.

Key words. cosmic microwave background – cosmic background radiation – large-scale structure of Universe – recombination

1. Introduction

This paper seeks to study the fundamental cosmology of our Universe and its early evolution, from right after inflation to the present day at very large scales. Our main tool for doing so is the Cosmic Microwave Background (CMB), and its physical properties. The study is based on the methodology suggested by Callin (2006).

This paper uses the Einstein equations and various results from statistical thermodynamics to derive numerical equations describing first a simple ΛCDM cosmology, and then seed this cosmology with initial perturbations, which theory tells us will be sourced from inflation. Evolution of these perturbations leads to observable anisotropies in the CMB, which will be reflected when we derive the CMB (and matter) power spectrum. The physical basis for doing this is supported by Dodelson (2003), and the specific methodology and formalism is described by Winther (2024).

The main goal is thus to be able to predict the CMB (and matter) fluctuations via the power spectrum from first principles. By being able to match observational data, we prove that our initial assumptions are reasonable and can apply for the real universe, such as inflation. By removing the impact of inflation or altering various cosmological parameters (like removing dark matter) from our simulation, we can produce results irreconcilable with observational data, which indicates that our universe includes these effects - or that the theory of relativity is incorrect, which seems unlikely to say the least.

The process of deriving the equations and then numerical implementation is a great tool to learn about the intricacies of modern cosmology (Callin 2006).

This study is baselined on the common Lambda-CDM model (chap. 1 Dodelson & Schmidt 2021, sec. 1.6), with a Friedmann-Robertson-Walker metric for spacetime.

2. Milestone I

In this milestone, we establish the so-called background cosmology of our universe for the simulation. We focus on some rough supernova fitting to give an initial target for the spacetime metric and relative energy densities we will work with.

Citations: Baumann (2017), Dodelson (2003) and (Callin 2006; Winther 2024; Hu et al. 1998)

2.1. Theory

The scale factor a is used as the main time-ish variable - a is not a time but since time, size of the universe, and cosmic distances are all closely related it can fulfill the role of a time variable nonetheless, and describe the evolution of our simulated universe (Winther 2024). The scale factor is a dimensionless quantity.

For numerical work we use the variable $x \equiv \log a$, this is for numerical stability over large timescales with highly variable quantities.

We also consider the cosmic time t, and in theory a is dependent on t, $a(t)$, but in practice we derive the cosmic time t from x (and thus a) and not the other way around, see eq. 5.

We define a_0 as the value of the scale factor today, such that $a_0 \equiv a(t_{\text{today}}) \equiv 1$. Note that $x_0 = 0$. In general, subscript $_0$ indicates the value of a parameter as measured in the current day.

Another related quantity is the redshift z, this is also $z_0 = 0$ in the present day. As observers we must by definition be at zero redshift, after all. Redshift is given by $1 + z = a_0/a(t) = 1/a$.

Fiducial cosmology and initial parameter values taken from the Planck 2018 results (Collaboration et al. 2020). Input parameters are listed at 1.

$$
\begin{aligned}
h &= 0.67, \\
T_{\mathrm{CMB0}} &= 2.7255\,\mathrm{K}, \\
N_{\mathrm{eff}} &= 3.046, \\
\Omega_{\mathrm{b0}} &= 0.05, \\
\Omega_{\mathrm{CDM0}} &= 0.267, \\
\Omega_{k0} &= 0, \\
\Omega_{\gamma 0} &= N_{\mathrm{eff}} \cdot \frac{7}{8}\left(\frac{4}{11}\right)^{4/3} \Omega_{\gamma 0}, \\
\Omega_{\Lambda 0} &= 1 - (\Omega_{k0} + \Omega_{b0} + \Omega_{\mathrm{CDM0}} + \Omega_{\gamma 0} + \Omega_{\nu 0}), \\
n_s &= 0.965, \\
A_s &= 2.1 \cdot 10^{-9}, \\
Y_p &= 0.245, \\
z_{\mathrm{reion}} &= 8, \\
\Delta z_{\mathrm{reion}} &= 0.5, \\
z_{\mathrm{He-reion}} &= 3.5, \\
\Delta z_{\mathrm{He-reion}} &= 0.5.
\end{aligned}
\tag{1}
$$

2.1.1. Friedmann equation

Rather than dealing with the full Einstein equations directly, it is possible to derive the Friedmann equation in order to describe the expansion of the universe, this is eq. 2 (Winther 2024).

$$
\boxed{H = H_0 \sqrt{\Omega_{M0} a^{-3} + \Omega_{R0} a^{-4} + \Omega_{k0} a^{-2} + \Omega_{\Lambda 0}}}, \tag{2}
$$

where the Ω_X are density parameters describing relative density of their respective form of energy contributing to the expansion of the universe. Density parameters are dimensionless. Subscript $_0$ indicates a value for the universe of today, since we as observers are by definition at $x = z = 0$.

$\Omega_M = (\Omega_b + \Omega_{\mathrm{CDM}})$ is a composite density parameter describing non-relativistic matter (baryons and cold dark matter), and $\Omega_R = (\Omega_\gamma + \Omega_\nu)$ is a composite density term for radiation (photons and neutrinos). Ω_Λ is the density parameter for dark energy. Ω_k is a curvature term, and not properly an energy density. However, it contributes to the Friedmann equation as if it were a normal matter fluid with equation of state $\omega = -1/3$. This term prescribes negative curvature when < 0, positive curvature when > 0, and a spatially flat universe when $= 0$. Our universe is observationally confirmed to be very close to flat (Bennett et al. 2013), so this term should be close to 0.

The unit of H is slightly ambiguous, as in SI units both (km/s)/Mpc and the simplified $1/\mathrm{s}$ are used. The first way of writing the unit is more intuitive, as it relates to the change in velocity of distant galaxies based on their distance from the observer (us), aka Hubble's law. $1/\mathrm{s}$ is technically correct but interpreting the Hubble parameter as a frequency is not helpful. For the Friedmann equation and derived quantities, we mostly skip this problem by keeping H in "units of H", using the value of the Hubble parameter today (H_0) as a constant which gives the right units to any H that pops up.

For numerical work, we calculate the constant H_0 by adding the right units to a dimensionless constant h (eq. 3), which is commonly used and reported in the literature (Croton 2013). h is one of the input observables for our numerical simulation, so we use the 0.67 value reported by Planck 2018 (Collaboration et al. 2020).

$$
H_0 = 100 * h \ \ \mathrm{km\,s^{-1}\,Mpc^{-1}} \tag{3}
$$

2.1.2. More stuff

Paper with supernova fitting data Betoule et al. (2014).

Equation for critical density of the universe today 4

$$
\rho_{c0} \equiv \frac{3H_0^2}{8\pi G} \ \ \mathrm{kg\,m^{-3}} \tag{4}
$$

$$
t(x) = \int_0^a \frac{da}{aH} = \int_{-\infty}^{x} \frac{dx}{H(x)} \quad \text{[unit s, can convert to Gyr etc.]} \tag{5}
$$

2.2. Implementation details

We run a Markov chain Monte Carlo simulation on a large number of parameter combinations, in order to test numerical fitting to real supernova data. This ensures our background parameters and simulation is sensible, before we add perturbations to simulate a dynamic universe development through time.

2.3. Results

See figs. 1, 2, 3, 4, 5. Overall these figures seem ok, except that the supernova fitting in fig. 2 misses systematically, especially at the beginning. There is probably some bug involved, since the shape seems correct.

Best-fit parameters are Best h: 0.706857, Best H0: 70.6857 km/s/Mpc, Best OmegaM: 0.268287, Best OmegaK: 1.84807e-05, Best OmegaLambda: 0.731694519

Via the cosmic time, the calculated current age of the Universe is: $13.849 * 10^9$ yrs. This is pretty close to 13.79 billion years, the current accepted estimate.

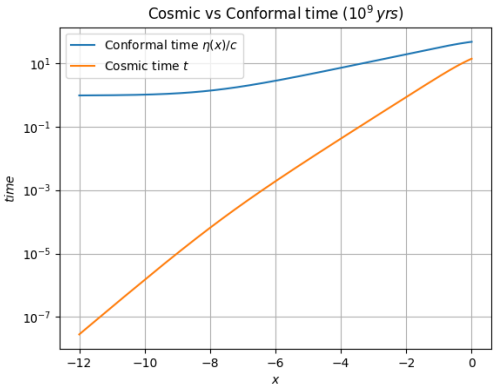

Fig. 1: Cosmic and conformal time plotted against the expansion of the universe. The cosmic time evolves almost linearly, as we'd expect.

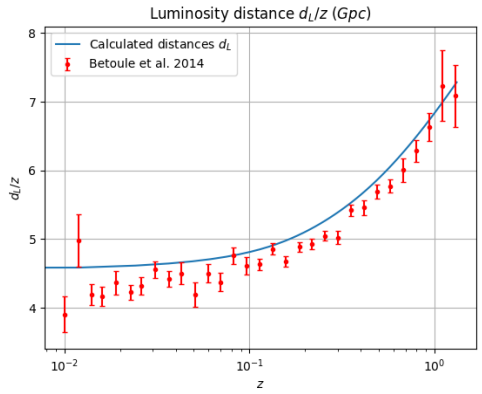

Fig. 2: Luminosity distance against redshift, with larger redshifts representing objects further away. This evolution is strongly related to the Hubble parameter and Hubble's law.

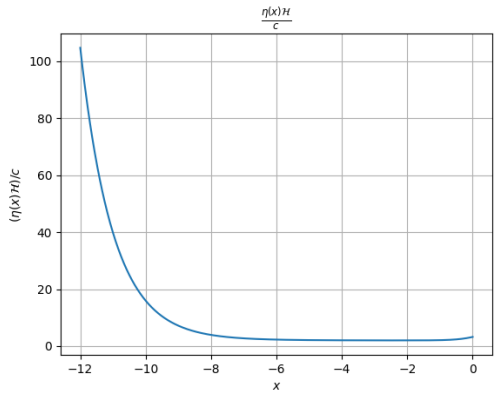

Fig. 3: A plot of the conformal Hubble factor $\mathcal{H} = aH$, scaled against the analytical solution of the Friedmann equation in the radiation dominated era ($\eta \simeq \frac{c}{\mathcal{H}}$). This should converge to 1 the more radiation dominated the universe is, and shows the correct exponential decay compared to the decay of relativistic matter seen in fig. 4, if not the right value at the beginning of the plot.

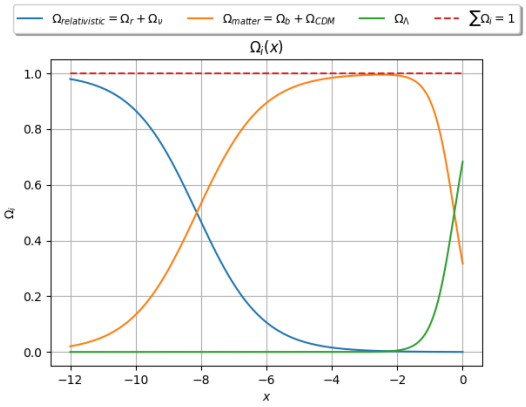

Fig. 4: The evolution of the various energy components from the Friedmann equation. We clearly see the three eras of radiation-domination, matter-domination, and dark energy beginning to dominate right around the present day, as expected. For reference, the sum of the components is calculated at every point and plotted at the top - this exeeding 100% energy at any point would be very problematic, but it stays perfectly at 1.

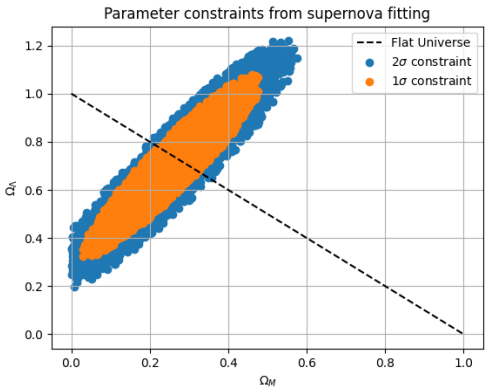

Fig. 5: A scatter plot of the various parameter combinations that were attempted for fitting by the MCMC. Parameters outside the blue area are extremely unlikely. For reference, the combinations corresponding to a spatially flat universe are the ones on the dotted black line. Since we know observationally that our universe is close to flat, a dark energy content of about 60-80% is likely, with a corresponding matter density of about 20-40%.

3. Milestone II

With fundamental cosmology established in sec. 2, we can now describe the baseline or so-called "background" behaviour of our universe, with a relatively simple evolution of cosmological parameters as the universe expands (refer fig. 4). Now we wish to look backwards from our current time, and compute the path of photons travelling towards a current-day observer from the early universe.

In order to study the behaviour of photons and thermal evolution of the early universe, we consider it to be a large continuous fluid, specifically a hot plasma. The thermodynamics and statistical mechanics for this are described in Baumann (2017, chap. 3) and Dodelson (2003, chap. 3, 4), while the specific Boltzmann formalism utilized is that of Winther (2024), available here.

3.1. Theory

Considering the early universe, there are three main interactions between particle species of interest, Couloumb scattering (6), Thomson scattering (7), and the formation/ionization of Hydrogen (8).

$$e^- + p^+ \rightleftharpoons e^- + p^+ \tag{6}$$
$$e^- + \gamma \rightleftharpoons e^- + \gamma \tag{7}$$
$$e^- + p^+ \rightleftharpoons H + \gamma \tag{8}$$

Start with eqs. 9 (Dodelson 2003, sec. 4.4) and 10.

$$\tau(\eta) = \int_\eta^{\eta_0} n_e \sigma_T a d\eta' \quad \text{[dimensionless]} \tag{9}$$

$$\boxed{\tau' = \frac{d\tau}{dx} = -\frac{c n_e \sigma_T}{H}} \quad \text{[dimensionless]} \tag{10}$$

Also the visibility function 11.

$$\tilde{g}(x) = \frac{d}{dx}e^{-\tau} = -\tau' e^{-\tau}, \quad \text{by def.} \int_{-\infty}^{0} \tilde{g}(x)dx = 1 \tag{11}$$

We wish to compute the fractional electron density given by 12, where we assume all baryons are protons and there are no heavier elements. This approximation is acceptable for getting a simple reionization with clear falloff of electrons as they get absorbed into hydrogen atoms. By including ionization into Helium, our resulting ionization plot would have multiple bumps for ionization into different states of Hydrogen+Helium.

$$\boxed{X_e \equiv n_e/n_H}, \text{ with } n_H = n_b \approx \frac{\rho_b}{m_H} = \frac{\Omega_{b0}\rho_{c0}}{m_H a^3} \tag{12}$$

In order to calculate the electron density, we can use the Saha approximation given in eq. 13. This is valid for large temperatures T, early in the universe. However, as the temperature falls the Saha approximation continues to predict a simple exponential decay of free electrons as they all become bound to hydrogen (and heavier elements), but this assumes the interaction 8 continues to be perfectly efficient, which is not the case in practice. See fig. 3.8 in Baumann (2017, sec. 3.3.3). We seek to recreate this figure with a numerical simulation.

$$\boxed{\frac{X_e^2}{1-X_e} = \frac{1}{n_b}\left(\frac{m_e T_b}{2\pi}\right)^{3/2} e^{-\frac{\epsilon_0}{k_b T_b}}} \quad [X_e \text{ dimensionless}] \tag{13}$$

In order to properly simulate the change in electron density, we can switch to the more accurate Peebles equation given as eq. 14 (Peebles 1968; Zel'dovich et al. 1969), with supporting definitions in eq. C. This equation is numerically unstable when solved for very large T (early on), but is perfectly appropriate around when the Saha approximation stops being accurate.

$$\boxed{\frac{dX_e}{dx} = \frac{C_r(T_b)}{H}\left[\beta(T_b)(1-X_e) - n_H \alpha^{(2)}(T_b) X_e^2\right]} \tag{14}$$

$[X_e \text{ dimensionless}]$

We will also calculate the so-called "sound horizon at decoupling", the total distance a sound-wave in the primordial photon-baryon plasma can propagate from the Big Bang until photons decouple. Pure photons have a sound speed $c/\sqrt{3}$, while sound-waves in the primordial plasma follow the slightly lower $c_s = c\sqrt{\frac{R}{3(1+R)}}$, with $R = \frac{4\Omega_{\gamma 0}}{3\Omega_{b0}a}$. Thus we end up with the sound-horizon given in eq. 15.

$$\boxed{s(x) = \int_0^a \frac{c_s dt}{a} = \int_{-\infty}^{x} \frac{c_s dx}{\mathcal{H}} \rightarrow \frac{ds(x)}{dx} = \frac{c_s}{\mathcal{H}}}, \tag{15}$$

$$\text{with } s(x_{\text{ini}}) = \frac{c_s(x_{\text{ini}})}{\mathcal{H}(x_{\text{ini}})} \quad [\text{unit m}]$$

3.2. Implementation details

3.3. Results

See figs. 6, 7, 8, 9, 10.

Simulated recombination happens at $x = -3.452$, giving a recombination time (cosmic time) of 96 273 898.543 years. This corresponds to a redshift $z = 33.908$. However, the actual expected redshift should be $z = 1100$, and the age of the universe 378 000 years, so this is extremely late. This is also visible from plots like fig. 6. I have not figured out where the bug is for this one, but it affects all later plots.

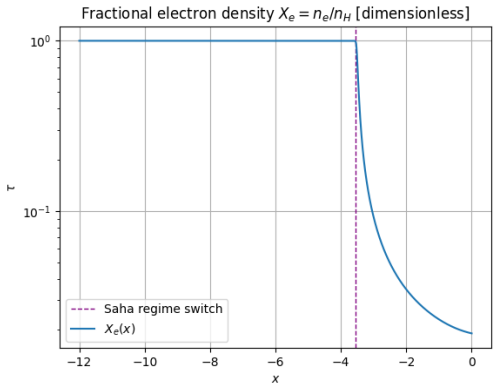

Fig. 6: Fractional electron density. Early times with density about 1 correspond to a high-energy universe where any hydrogen that forms instantly gets reionized by random photons. We see the expected exponential drop once the temperature has dropped sufficiently and recombination kicks in, with the dampening provided by Peebles making X_e converge to some non-zero value as the likelihood of proton-electron interactions drop. This would not be modelled by a simple implementation of just the Saha approximation. However, the extremely late recombination is unexpected, so the electron fraction does not seem to have stabilized by the present day which cannot be correct.

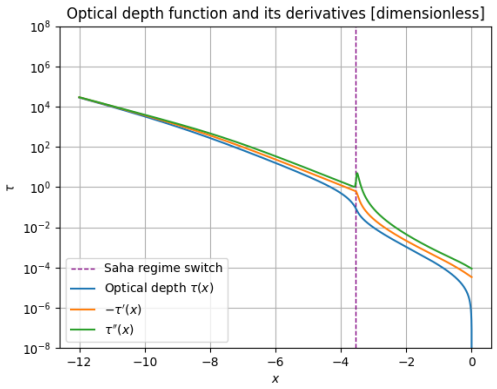

Fig. 7: The optical depth function and its derivatives, which evolves as expected, falling steadily as the universe expands until recombination, which is adequately represented by the point where we switch from the Saha approximation, noted in the plot. The bump in optical density is provided by all the new hydrogen forming. However, the falloff once the universe becomes transparent is not as sharp as expected, and recombination happens too late anyway.

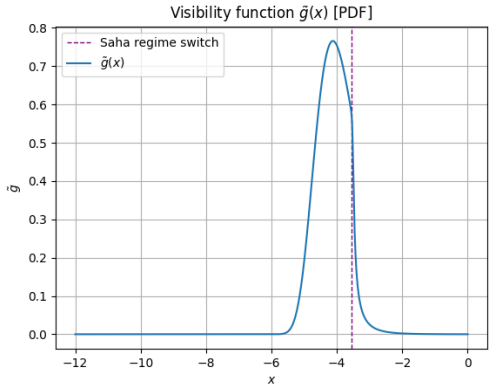

Fig. 8: The visibility function is a probability density function (and thus the integral sums to 1, which lines up with what we see), and represents the likelihood that a photon was last scattered at time x before free flying to hit a modern-day observer. The clear peak corresponds to recombination, where the universe becomes transparent as free electrons are bound into hydrogen, and represents the surface of last scattering. It is very unlikely that photons before this point flew unimpeded, as they likely scattered off the dense medium before this (see fig. 7). However, the peak is not quite as defined as expected.

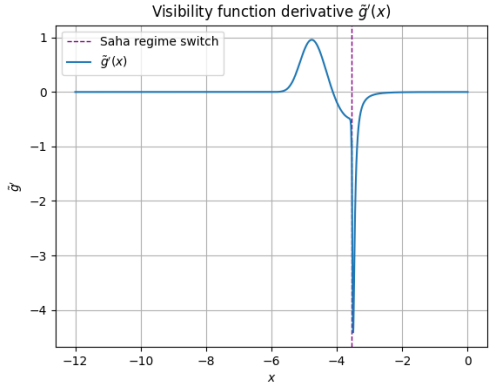

Fig. 9: First derivative of the visibility function. Has the expected rough shape.

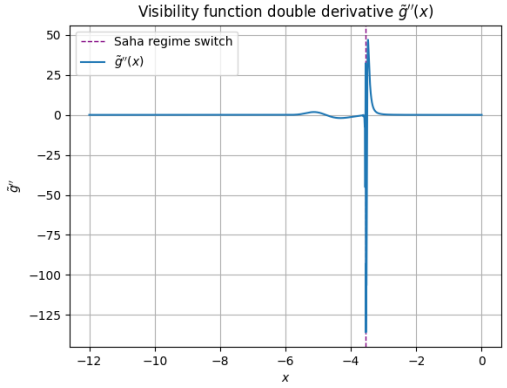

Fig. 10: Second derivative of the visibility function. This one looks weird, especially the early bump around $x = -5$.

4. Milestone III

Now we introduce density perturbations to our baseline cosmology, and study the evolution of these perturbations. Perturbations apply to photon multipoles, baryon and dark matter density and velocity, and to the gravitational metric.

Citations: Ma & Bertschinger (1995)

4.1. Theory

We can derive a system of ODEs to solve in order to study perturbations. See Winther (2024, part 3, cosmological perturbation theory) for derivation of these equations. The main equations to solve are eqs. 16 and 17, for matter perturbations (CDM, baryons) and perturbations of the graviational metric respectively.

$$\begin{aligned}
\delta'_{\mathrm{CDM}} &= \frac{ck}{\mathcal{H}} v_{\mathrm{CDM}} - 3\Phi' \\
v'_{\mathrm{CDM}} &= -v_{\mathrm{CDM}} - \frac{ck}{\mathcal{H}}\Psi \\
\delta'_b &= \frac{ck}{\mathcal{H}} v_b - 3\Phi' \\
v'_b &= -v_b - \frac{ck}{\mathcal{H}}\Psi + \tau' R(3\Theta_1 + v_b)
\end{aligned} \tag{16}$$

$$\begin{aligned}
\Phi' &= \Psi - \frac{c^2k^2}{3\mathcal{H}^2}\Phi + \\
&+ \frac{H_0^2}{2\mathcal{H}^2}\left[\Omega_{\mathrm{CDM}0} a^{-1}\delta_{\mathrm{CDM}} + \Omega_{b0} a^{-1}\delta_b + 4\Omega_{\gamma 0} a^{-2}\Theta_0\right] \\
\Psi &= -\Phi - \frac{12H_0^2}{c^2k^2a^2}\left[\Omega_{\gamma 0}\Theta_2\right]
\end{aligned} \tag{17}$$

R is the same as earlier, $R = \frac{4\Omega_{\gamma 0}}{3\Omega_{b0}a}$.

However, these equations are affected by the temperature and photon hotspots in the fluid we are considering to be the universe. Photons, unlike baryons, have multipolar effects, which enter as Θ_ℓ. Each Θ_ℓ depends on $\Theta_{\ell+1}$, which makes for an infinite set of equations to solve. Thankfully, line of sight integration as developed by (Zaldarriaga and Seljak) can solve this problem, providing an alternate means of calculating a power spectrum from the Boltzmann equations we started with. (See lecture notes citation). Line of sight integration only needs a few starting multipoles for verification, so in this project we will truncate the multipole hierarchy at around six.

Apart from photon multipoles, there are also additional effects from both neutrino multipoles and polarization of the photon fluid. These will not be treated in this project, instead see for example (something where they actually do it). But here, we treat $\mathcal{N}_\ell = 0$ and $\Theta_\ell^P = 0$.

The equations for photon multipoles to be included are eq. 18.

$$
\begin{aligned}
\Theta_0' &= -\frac{ck}{\mathcal{H}}\Theta_1 - \Phi' \\
\Theta_1' &= \frac{ck}{3\mathcal{H}}\Theta_0 - \frac{2ck}{3\mathcal{H}}\Theta_2 + \frac{ck}{3\mathcal{H}}\Psi + \tau'\left[\Theta_1 + \frac{1}{3}v_b\right] \\
\Theta_\ell' &= \frac{\ell ck}{(2\ell+1)\mathcal{H}}\Theta_{\ell-1} - \frac{(\ell+1)ck}{(2\ell+1)\mathcal{H}}\Theta_{\ell+1} \\
&\quad + \tau'\left[\Theta_\ell - \frac{1}{10}\Pi\delta_{\ell,2}\right], \quad 2 \le \ell < \ell_{\max} \\
\Theta_\ell' &= \frac{ck}{\mathcal{H}}\Theta_{\ell-1} - c\frac{\ell+1}{\mathcal{H}\eta(x)}\Theta_\ell + \tau'\Theta_\ell, \quad \ell = \ell_{\max}
\end{aligned}
\tag{18}
$$

4.2. Implementation details

4.3. Results

See figs. 11, 12, 13, 14, 15, 16.

Recombination happened too late, and whatever was going on there seems to have severely interfered with these results. No time to investigate properly, though. Presumably the pipeline is fine and just needs fixes to the calculations, and then these plots would turn out as they should.

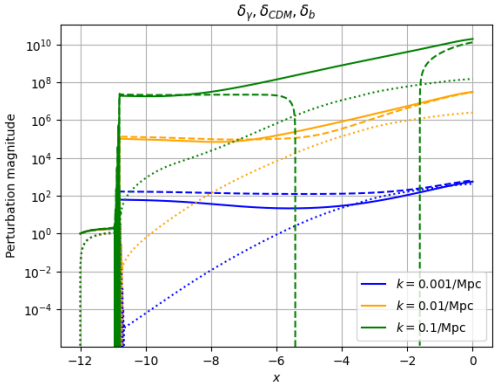

Fig. 11: Perturbations to densities, represented by the parameter δ presented by Winther (2024). CDM perturbations are represented by the solid line, baryon perturbations by the dashed line, and photon perturbations by the dotted line. Photon perturbations evolve mostly unaffected by the matter perturbations, which is good. Baryons might be oscillating away from the dark matter (due to baryon dragging) as expected, but fall off the scale of the plot. Early time development is completely messed up. Different scales might be entering evolution at different times as expected, but this is hard to tell.

5. Milestone IV

I got completely stuck on milestone III. I was looking forward to III and finally getting to some of the physics there, too

Citations: Fixsen et al. (1996)

5.1. Theory

CMB and matter power spectrums, how they work and the different regimes in them. How a sum of coefficients describes the different scale components of a sky-map. Line of sight integration to calculate all the various Θ_ℓ-s.

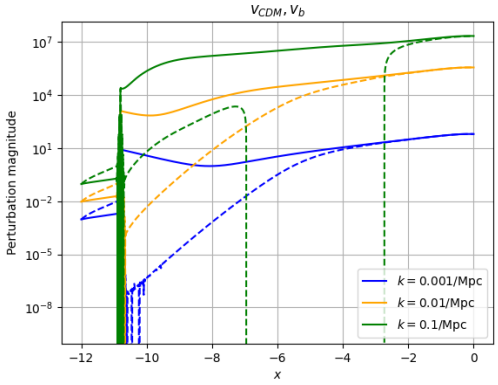

Fig. 12: Similar to fig. 11, but for perturbed average velocities of the respective quantities. Early times are completely messed up.

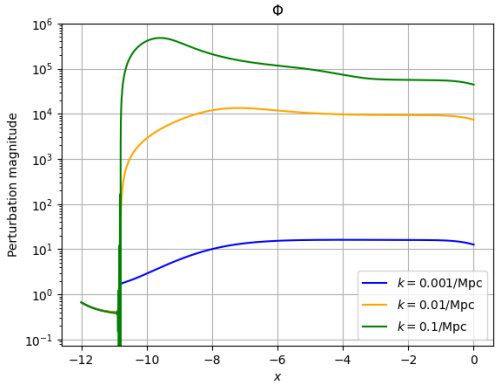

Fig. 13: Perturbations to the graviational metric, component Φ. The scale dependency is wrong, modes that enter early should fall off to zero much more aggressively. Perturbations should start around the same size and stay relatively constant until reentering the horizon. We do not observe the change in evolution as the universe starts to become dominated by dark energy at the very end.

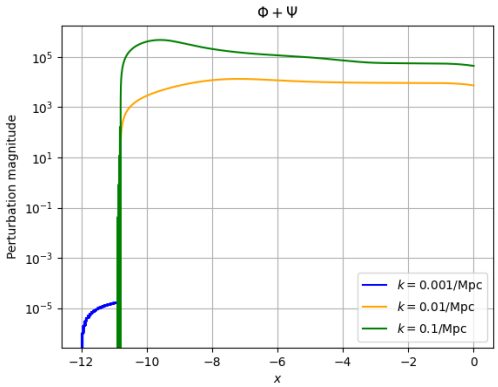

Fig. 14: Combined perturbations to the graviational metric. Same problems as fig. 13.

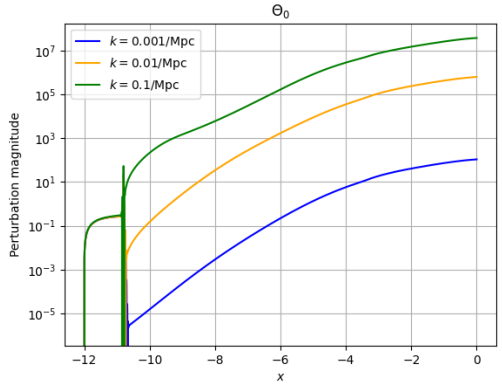

Fig. 15: The evolution of the photon monopole. Modes should be re-entering at different times to start a significant dampened oscillation, but the plot is messed up.

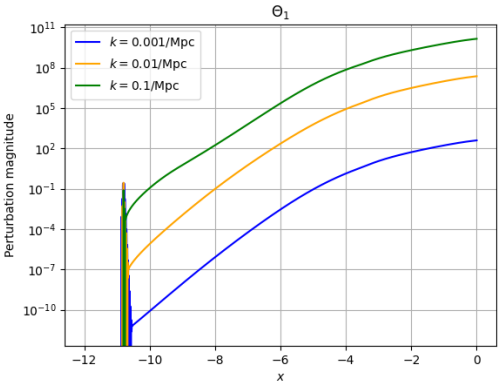

Fig. 16: Evolution of the photon dipole. Same problems as fig. 15.

How the different regimes in the power spectrum plots are affected by different shifts in cosmological parameters. Cosmic variance in the beginning at low ℓ-s. A_s for overall amplitude of the whole spectrum, n_s describes tilt. The fluctuation peaks after the main peak tell us about baryon and dark matter density. Also affected by polarization, neturinos, and reionization which is why the simpler power spectrum we would have derived would be off from the Planck spectrum in this regime, while the lower ℓ-s match fine.

The matter power spectrum tells us about the total matter component in the universe, but the interesting part is the second small peak and subsequent dampened fluctuations that tell us about the ratio of baryons to dark matter, due to the effect of baryon dragging.

The source function:

$$\tilde{S}(k,x) = \tilde{g}\left[\Theta_0 + \Psi + \frac{1}{4}\Pi\right] + e^{-\tau}\left[\Psi' - \Phi'\right] - \\ -\frac{1}{ck}\frac{d}{dx}(\mathcal{H}\tilde{g}v_b) + \frac{3}{4c^2k^2}\frac{d}{dx}\left[\mathcal{H}\frac{d}{dx}(\mathcal{H}\tilde{g}\Pi)\right]. \quad (19)$$

This describes various effects in the universe that have affected photons travelling from the surface of last scattering (the CMB photons) to us, today. The baseline movement is in the first term (hence the dependency on visibility function). The term with ψ dependence is a correction due to the Sachs-Wolfe effect, the term with Π is a correction for the effect of the photon quadropole and some polarization. The next main term is a correction for the integrated Sachs-Wolfe effect (ISW), which should have one of those neat diagrams to show how photons gain energy due to gravitational wells decaying while they are climbing out. Next up is a correction for Doppler shift, and finally a correction for angular dependence in Thompson scattering.

5.2. Implementation details, results

It did not work

6. Conclusions

This project provides a brisk walk through some important results for modern cosmology, but unfortunately falls short of finally getting the CMB power spectrum working.

1. The CMB power spectrum is an important tool for probing various cosmological parameters and both large-scale physics as well as early evolution of our universe.
2. Inflation is needed to source the distribution of matter in a way that can resemble our current universe.
3. Dark matter is needed to explain not just galaxy rotation curves, but also the overall behaviour of the CMB and matter power spectrums, along with effects like baryon dragging. Dark matter is not a simple numerical artifact but fundamentally needed to understand the development of modern cosmological models.
4. Array wrangling of complex implicit objects in Milestone III is not fun.

Acknowledgements.

References

Baumann, D. 2017, Lecture Notes for Cosmology, Part 3 Mathematical Tripos, https://cmb.wintherscoming.no/pdfs/baumann.pdf, (accessed 2025-02-17)
Bennett, C. L., Larson, D., Weiland, J. L., et al. 2013, ApJS, 208, 20
Betoule, M., Kessler, R., Guy, J., et al. 2014, A&A, 568, A22
Callin, P. 2006 [arXiv:astro-ph/0606683]
Collaboration, P., Aghanim, N., Akrami, Y., et al. 2020, A&A, 641, A6
Croton, D. J. 2013, Publ. Astron. Soc. Aust., 30, e052
Dodelson, S. 2003, Modern Cosmology, nachdr. edn. (Amsterdam: Academic Press)
Dodelson, S. & Schmidt, F. 2021, Modern Cosmology, second edition edn. (London San Diego, CA Cambridge, MA Oxford: Academic Press, an imprint of Elsevier)
Fixsen, D. J., Cheng, E. S., Gales, J. M., et al. 1996, ApJ, 473, 576
Hu, W., Seljak, U., White, M., & Zaldarriaga, M. 1998, Phys. Rev. D, 57, 3290
Ma, C.-P. & Bertschinger, E. 1995, ApJ, 455, 7
Peebles, P. J. E. 1968, Astrophys. J., 153, 1
Winther, H. A. 2024, Cosmology II: Lecture Notes, https://cmb.wintherscoming.no/literature.php, (accessed 2025-02-17)
Zel'dovich, Ya. B., Kurt, V. G., & Syunyaev, R. A. 1969, Sov. J. Exp. Theor. Phys., 28, 146

Appendix A: Code repository

All code used for this project is available at this Github repository. The src folder contains the numerical C++ code. Calculated results are in csv-files found under the results folder. Presentation is handled by Python scripts per milestone, in the respective Milestone X folders. Produced plots are saved to a Plots folder under each Milestone.

Appendix B: Milestone I, extra plots

Evolution of some physical quantities in figs. B.1 and B.2.

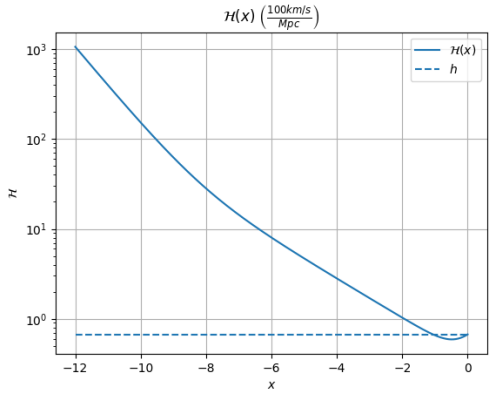

Fig. B.1: Direct plot of $\mathcal{H}$. For reference the current accepted value of h is plotted, which intercepts the plot as expected at $x = 0$. We see the expected steady falloff with a slight change in steepness as the universe becomes matter dominated, and a reversal in the size of H as the universe becomes dominated by dark energy.

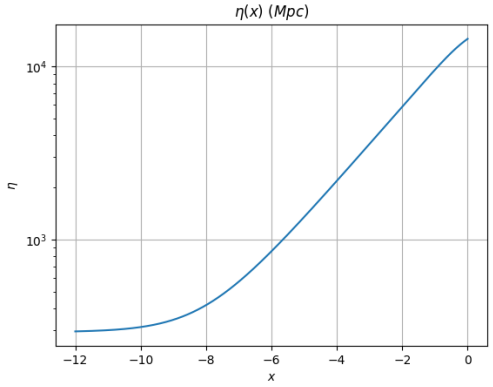

Fig. B.2: Direct plot of the conformal time. Relates to cosmic horizons, which expand slowly in the radiation dominated era.

Histograms of parameter distribution in fig. B.3.

Appendix C: Milestone II, extra math

Definitions to support Peebles equation (14):

$$C_r(T_b) = \frac{\Lambda_{2s\to 1s} + \Lambda_\alpha}{\Lambda_{2s\to 1s} + \Lambda_\alpha + \beta^{(2)}(T_b)}, \quad \text{[dimensionless]}$$

$$H, \quad [1/\text{s}]$$

$$\Lambda_{2s\to 1s} = 8.227, \quad [1/\text{s}]$$

$$\Lambda_\alpha = H\frac{(3\epsilon_0)^3}{(8\pi)^2 c^3 \hbar^3 n_{1s}}, \quad [1/\text{s}]$$

$$n_{1s} = (1 - X_e)n_H, \quad [1/\text{m}^3]$$

$$n_H = (1 - Y_p)n_b \approx (1 - Y_p)\frac{3H_0^2\Omega_{b0}}{8\pi G m_H a^3}, \quad [1/\text{m}^3]$$

$$\beta^{(2)}(T_b) = \beta(T_b)e^{\frac{3\epsilon_0}{4k_bT_b}}, \quad [1/\text{s}]$$

$$\beta(T_b) = \alpha^{(2)}(T_b)\left(\frac{m_e k_b T_b}{2\pi\hbar^2}\right)^{3/2} e^{-\frac{\epsilon_0}{k_bT_b}}, \quad [1/\text{s}]$$

$$\alpha^{(2)}(T_b) = \frac{8}{\sqrt{3\pi}} c\sigma_T \sqrt{\frac{\epsilon_0}{k_bT_b}}\phi_2(T_b), \quad [\text{m}^3/\text{s}]$$

$$\phi_2(T_b) = 0.448 \ln\left(\frac{\epsilon_0}{k_bT_b}\right), \quad \text{[dimensionless]}$$

$$\sigma_T = \frac{8\pi}{3}\left(\frac{\alpha\hbar c}{m_e c^2}\right)^2, \quad [\text{m}^2]$$

$$\alpha \simeq \frac{1}{137.0359992} \quad \text{[dimensionless, fine-structure constant]}$$

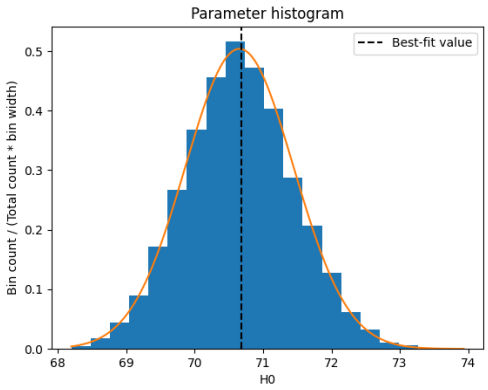

(a) Accepted samples for H_0.

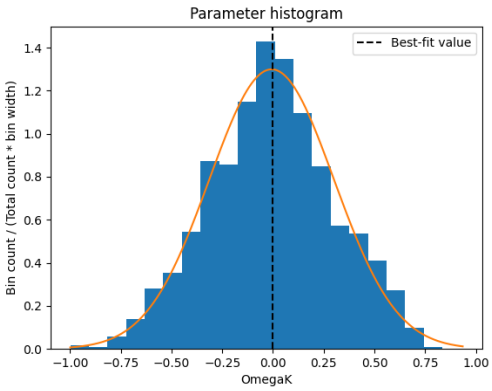

(b) Accepted samples for Ω_K.

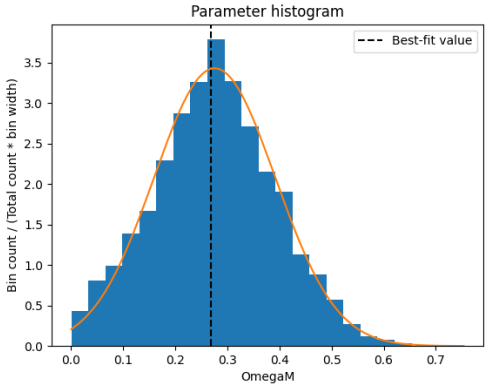

(c) Accepted samples for Ω_M.

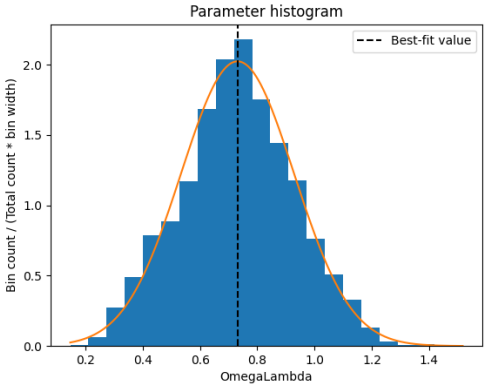

(d) Accepted samples for Ω_Λ.

Fig. B.3: Histogram of accepted samples from the MCMC, with a simple gaussian function with the same mean and standard deviation overplotted. Sampling covers a suitably random range and should be a good representation of possible parameter values. The final best-fit values are indicated.

Appendix D: Milestone III, extra math

Initial conditions for D.1:

$$
\begin{aligned}
\Psi &= -\frac{1}{\frac{3}{2} + \frac{2f_\nu}{5}} \\
\Phi &= -(1 + \frac{2f_\nu}{5})\Psi \\
\delta_{\rm CDM} &= \delta_b = -\frac{3}{2}\Psi \\
v_{\rm CDM} &= v_b = -\frac{ck}{2\mathcal{H}}\Psi \\
&\text{Photon multipoles:} \\
\Theta_0 &= -\frac{1}{2}\Psi \\
\Theta_1 &= +\frac{ck}{6\mathcal{H}}\Psi \\
\Theta_2 &= -\frac{20ck}{45\mathcal{H}\tau'}\Theta_1 \qquad \text{(without polarization)} \\
\Theta_\ell &= -\frac{\ell}{2\ell+1}\frac{ck}{\mathcal{H}\tau'}\Theta_{\ell-1}
\end{aligned}
\tag{D.1}
$$